JOURNAL OF MATERIALS SCIENCE 32 (1997) 295–300

Processing, microstructure and mechanical properties of hot-pressed SiC continuous fibre/SiC composites

K. PARK
Department of Materials Engineering, Chung-ju National University, Chung-ju, Korea
T. VASILOS
Department of Chemical and Nuclear Engineering, University of Massachusetts, Lowell, MA 01854, USA

SiC (SCS-6™) continuous fibre/SiC composites were fabricated by hot-pressing at 1700 °C in vacuum using an Al sintering additive. Analytical transmission electron microscopy was used to investigate the microstructure of the composites. The room-temperature mechanical and high-temperature creep properties of the composites were investigated by four-point bending. The SiC powders used were sintered at a relatively low sintering temperature to high density (97% of theoretical density) with the addition of the Al sintering additive. It is believed that the Al additive is very efficient for the densification of SiC. The SiC fibres maintained their original form and microstructure during fabrication. The SiC matrix reacted with the outermost carbon sublayer in the fibre, forming a thin (1.8–4.8 μm) interfacial layer, which was composed of Al_4C_3, Si–Al–C, and Si–Al–O phases. The incorporation of SiC fibre into a dense SiC matrix significantly increased the room-temperature failure strain and improved the high-temperature creep properties. In addition, the incorporation of SiC fibre into a porous SiC matrix increased the room-temperature failure strain, but did not contribute to the high-temperature creep properties.

1. Introduction

Silicon carbide (SiC) possesses excellent high-temperature strength, stiffness, oxidation resistance, and low density and can be fabricated at low cost, making it a prime candidate for high-temperature structural applications. However, SiC is extremely brittle so that it fails in a brittle fashion with very little deformation to failure. This can be a major problem when it is utilized in weight-bearing areas of structural applications. Fibre-reinforcement is a promising strategy for strengthening SiC. In the present study, an attempt is made to improve the fracture toughness of SiC by the incorporation of SiC (SCS-6™) continuous fibre (Textron Specialty Materials, Lowell, MA 01851, USA) in a unidirectional array. The SiC fibre is an important reinforcement for ceramic- and metal-matrix composites, due to its high tensile strength (3450 MPa), high tensile modulus (400 GPa), and low density (3.0 g cm^{-3}) [1].

Generally, the densification of pure SiC is extremely difficult because of its covalent nature. Therefore, several sintering additives, such as C [2, 3], B [2–4], Al [3, 5], Al_2O_3 [6, 7], B_4C [7], B and C [2, 3], and B and Al [4], have previously been used to fabricate fully dense SiC. In this work, an Al sintering additive was chosen to facilitate a low densification-temperature in order to minimize the SiC fibre degradation. Two kinds of SiC (SCS-6™) fibre/SiC composites were fabricated by hot-pressing under different applied pressures of 31.0 and 20.7 MPa in vacuum using the Al sintering additive. The purpose of this study was to investigate the microstructure of the composites and to understand the role of the Al additive on the composites and also investigate the relationship between the microstructural features and mechanical properties.

2. Experimental procedures

The materials used in this study were (1) commercial-grade β-SiC powder (Superior Graphite Co., Chicago, IL), (2) SCS-6™ SiC fibre, and (3) Al metal powders (Aluminium of America, Pittsburgh, PA) as a sintering additive. The β-SiC and Al (5 wt%) powders were mixed in a polyethylene mill jar with ethyl alcohol, to form a slurry which was milled for 8 h using Si_3N_4 balls and was then dried in a drying oven. To break up agglomerates, the dried mixtures were ball-milled for 5 min. The SiC fibres were wound onto plastic foils with a linear density of 6 fibres per mm in a unidirectional array and then fixed using a sprayed Krylon type adhesive in order to avoid contact between the fibres. The fibre foils were dried and then cut into small sections (54 × 54 mm). The dried mixtures of SiC and Al powders were spread between the fibre foils in the press die cavity (54 × 54 mm). The die cavity and punch were coated with a thin layer of boron nitride (BN) in order to avoid reaction with the graphite die.

0022–2461

Subsequently, two kinds of SiC fibre/SiC composites were fabricated by hot-pressing at 1700 °C under different applied pressures of 31.0 and 20.7 MPa for 1 h in vacuum. The composites fabricated at applied pressures of 31.0 and 20.7 MPa are denoted as composite A and B, respectively. The composites A and B contained 22 and 18 vol% SiC fibre, respectively. The composites were cooled to room temperature and then machined into rectangular bars ($3 \times 4 \times 45$ mm), in which the fibres were parallel to the longitudinal direction.

The microstructural information on the composites was obtained from transmission electron microscopy (TEM). Cross-sectional TEM specimens were sectioned perpendicular to the fibre with a low-speed diamond saw and mechanically ground to ~ 300 μm. Circular discs of 3 mm in diameter of the specimens were core drilled from the ground sections. The specimens were mechanically ground to ~ 120 μm, and then dimpled to ~ 30 μm. The specimens were ion milled with 5 kV Ar^+ ions at an incident angle of 12° until perforation was achieved. A light carbon film was evaporated onto the specimens in order to prevent charging in the electron microscope. The microstructure and chemistry of the specimens were investigated by a bright field image, selected area diffraction (SAD), convergent beam electron diffraction (CBED), and energy dispersive X-ray spectroscopy (EDS) using a Philips EM400T TEM and a Noran ultrathin window Micro-Z detector. The room-temperature mechanical properties of the composites were measured at a crosshead speed of 0.5 mm per min by four-point bending in accordance with ASTM standards D790 [8] and E4 [9] using an Instron universal testing machine. In addition, the high-temperature creep behaviours of the composites were investigated by four-point bending at 1100 °C and a bending stress of 100 MPa for 48 h in air.

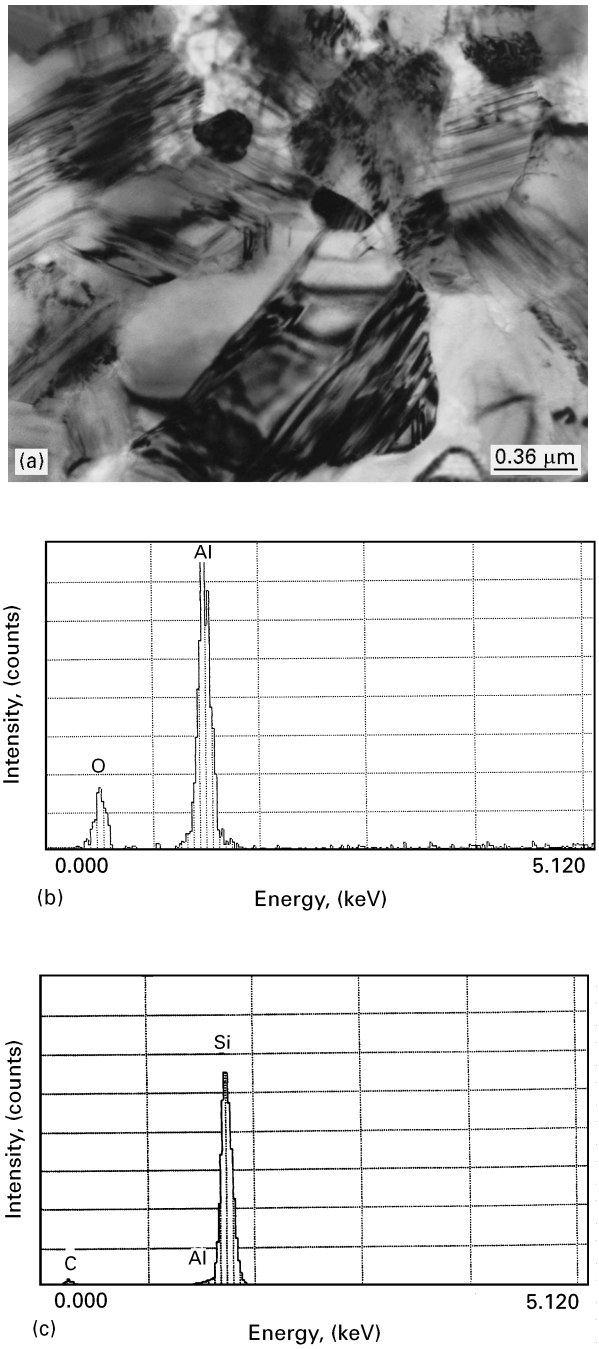

Figure 1 (a) Bright field image of SiC matrix in composite A. (b) EDS spectrum obtained from Al-rich second phase (Al_2O_3) formed at the matrix grain boundaries. (c) EDS spectrum obtained from the matrix having a small amount of Al, forming SiC–Al solid solutions.

3. Results and discussion

3.1. SiC fibre (22 vol%)/SiC composite fabricated at an applied pressure of 31.0 MPa (composite A)

3.1.1. Microstructure

The SiC matrix in composite A was dense (97% of theoretical density) and fine-grained and contained many twins within the grains, as shown in Fig. 1(a). An Al-rich second phase (e.g., Al_2O_3) was found at the matrix grain boundaries, Fig. 1(b). The grain boundary phase was probably responsible for the densification of the SiC powders. The SiC matrix contained a small amount of Al (Fig. 1(c)) producing SiC–Al solid solutions. The solubility of Al in SiC at 2200 °C has been reported as 1.0 wt% [10]. These results are consistent with the observation reported by Hamminger *et al.* [11], who found that most of the Al was segregated at the SiC grain boundaries and a little Al was present within the SiC grains. The SiC matrix existed mainly as β-SiC with a cubic structure ($a = 0.435$ nm) and sometimes as α-SiC with a hexagonal structure (4H, 6H, or 8H).

The SiC fibre in composite A was uniformly distributed through the matrix. The microstructure of the fibre, which had undergone relatively high-temperature (1700 °C) exposure during fabrication, was investigated. It was found that the fibre was undamaged by the fabrication, thus clearly showing several different layers (core carbon, inner carbon layer, SiC layer, and outer carbon layer) similar to the unprocessed single SiC (SCS-6™) fibre reported by Ning and Pirouz [12]. Fig. 2(a) shows a bright field image of a core carbon, inner carbon, and SiC layer in the SiC fibre. The microstructure of the SiC layer with columnar grains was identified as β-SiC with a cubic

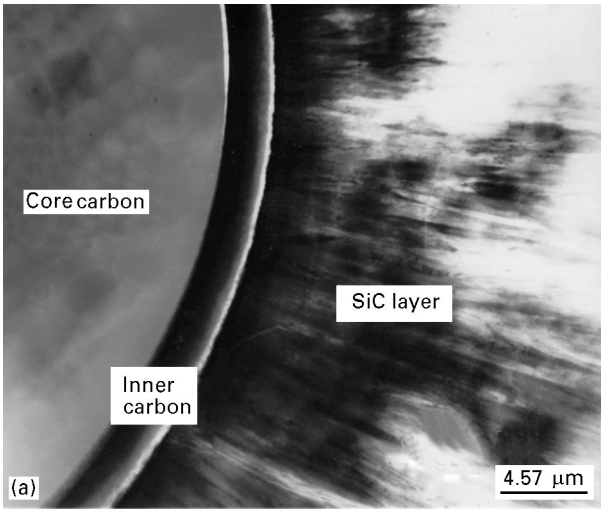

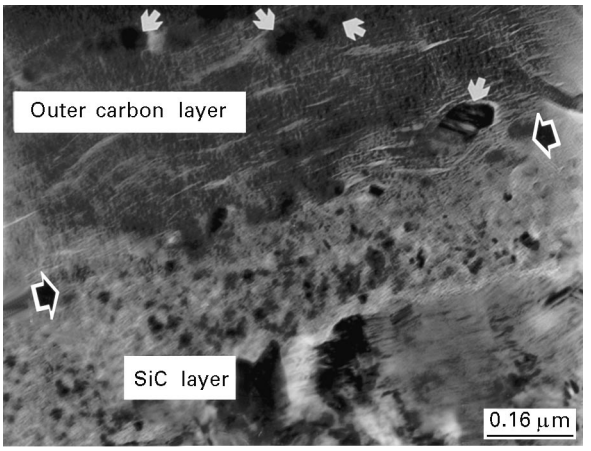

Figure 3 Bright field image of small equiaxed SiC grains grown on the outside of the columnar SiC grains in the SiC fibre.

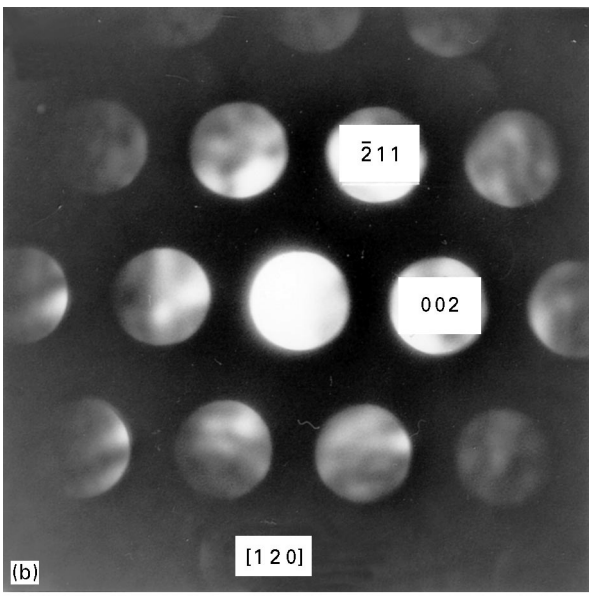

Figure 2 (a) Bright field image of a core carbon, inner carbon, and SiC layer in the SiC fibre (composite A). (b) CBED pattern obtained from the SiC layer.

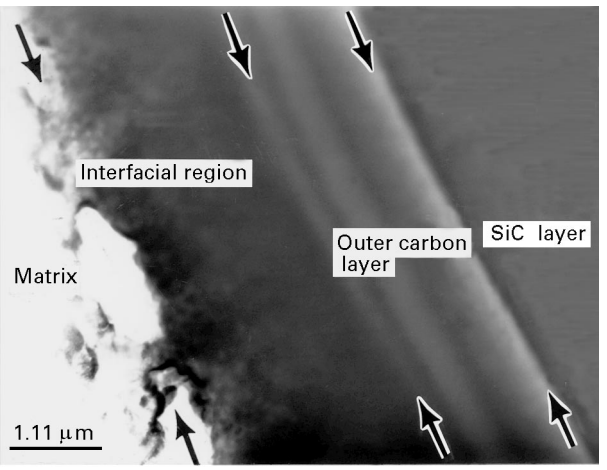

Figure 4 Bright field image of an interfacial region between the SiC matrix and the outermost carbon layer in the SiC fibre (composite A).

structure, Fig. 2(b). Small equiaxed SiC grains were grown on the outside of the columnar SiC grains before the growth of the outer carbon layer, as shown in Fig. 3. In the outer carbon layer, SiC particles (indicated by arrows) were embedded within carbon. The outer carbon layer was designed to protect the SiC layer against damage due to the interfacial reaction with the matrix and to relieve stress concentration at the surface of the SiC layer. It also serves as a mechanical de-bonding layer between the matrix and fibre [13].

In an attempt to determine the nature of the reaction between the fibre and matrix during fabrication, the interfacial region between these two components was investigated. It was found that the outermost carbon sublayer in a SiC fibre reacted with the matrix during fabrication to produce a thin interfacial region (1.8–4.8 μm). Fig. 4 shows a bright field image of an interfacial region between the outermost carbon sublayer and the matrix. The thicknesses of the outermost carbon sublayer and matrix interacted are ~ 0.56 and ~ 1.68 μm, respectively. In order to investigate the microstructure of the interfacial region in detail, a bright field image of the interfacial region was obtained at high magnification, Fig. 5(a). The interface between the interfacial region and outermost carbon sublayer was relatively sharp, while the interface between the interfacial layer and matrix was usually wavy. Most of the interfacial region was Al_4C_3 with a rhombohedral structure ($a = 0.334$ nm and $c = 2.499$ nm), Fig. 5(b), which shows a SAD pattern obtained from the Al_4C_3 which was formed by the following chemical reactions: $4Al + 3C = Al_4C_3$ [14] and $3SiC + 4Al = Al_4C_3 + 3Si$ [15]. A small amount of Si was often detected near the Al_4C_3.

An Al_2SiO_5 phase with an orthorhombic structure ($a = 0.779$ nm, $b = 0.789$ nm, and $c = 0.556$ nm) was formed at a weak interface between the interfacial layer and matrix. The weak interface is desirable for good fracture toughness because it makes the crack initiated in the matrix deflect around the SiC fibres and thus inhibits its propagation through the fibres. Fig. 5(c) shows a CBED pattern obtained from the Al_2SiO_5. It is important to note that some separations were often observed at the interface between the interfacial region and outermost carbon sublayer. These

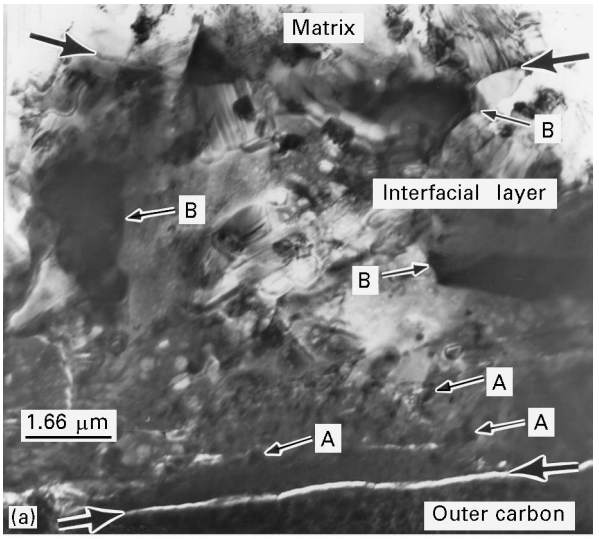

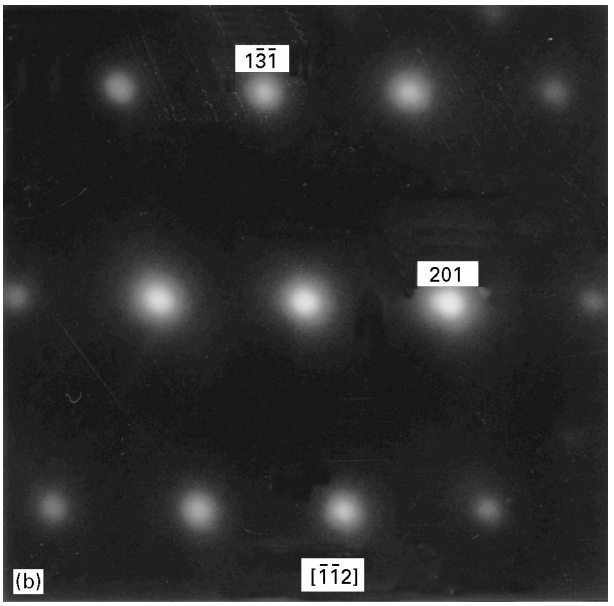

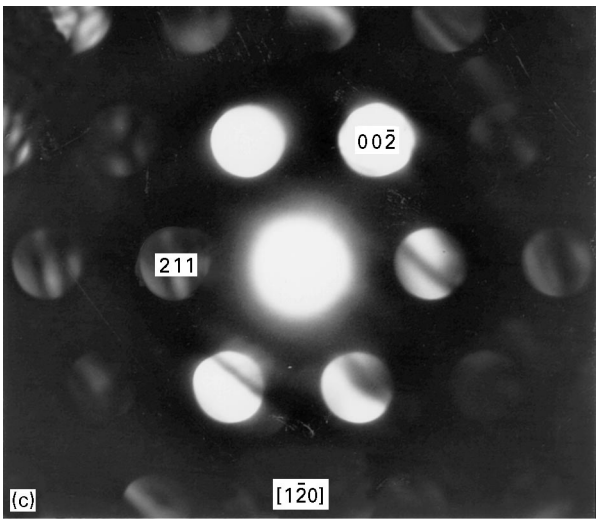

Figure 5 (a) Magnified bright field image of an interfacial region between the SiC matrix and the outermost carbon sublayer in the SiC fibre (composite A). The Si–Al–C and Si–Al–O phases in the interfacial region are indicated by A and B, respectively. (b) SAD pattern obtained from Al_4C_3 phase in the interfacial region. (c) CBED pattern obtained from Al_2SiO_5 phase in the interfacial region.

separations were responsible for the decrease in fracture strength. In addition, Si–Al–C and Si–Al–O phases were present at the inside and outside of the interfacial region, respectively. In Fig. 5(a), the Si–Al–C and Si–Al–O phases present in the interfacial region are indicated by A and B, respectively. The Si–Al–C phase could be formed by chemical reaction between Al and SiC [16] and also Al_4C_3 and SiC [14]. At present, the origin of the Si–Al–O phase and the crystalline structure of the Si–Al–C and Si–Al–O phases are not determined.

3.1.2. Room-temperature mechanical properties and high-temperature creep properties

The room-temperature mechanical properties of composite A and monolithic SiC with the same porosity as composite A are shown in Fig. 6. The incorporation of SiC fibre into a SiC matrix resulted in an increase in the strain to failure and a decrease in the fracture strength, relative to the monolithic SiC. The weak bonding between the interfacial region and matrix contributed to a significant increase in the strain to failure because of crack deflections around the fibres. The decrease in fracture strength could result from separations between the interfacial region and outermost carbon sublayer. Fig. 7 shows a deflection–time behaviour of the composite A and monolithic SiC with the same porosity as composite A, measured at 1100 °C and a bending stress of 100 MPa for 48 h. The composite A shows a lower strain rate and deflection than the monolithic SiC, indicating the benefit of fibre additions. The improvement in high-temperature creep properties could result from the fact that grain boundary sliding in the matrix was hindered by the fibres and also that deformation in the matrix was restrained by the fibres.

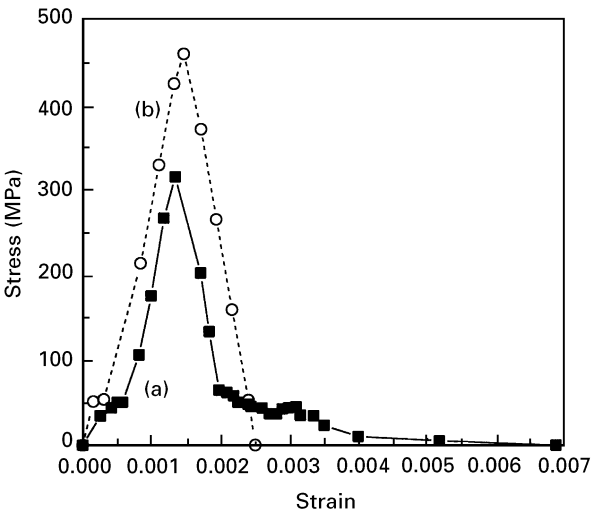

Figure 6 Room-temperature mechanical properties of (a) composite A and (b) monolithic SiC with the same porosity as composite A.

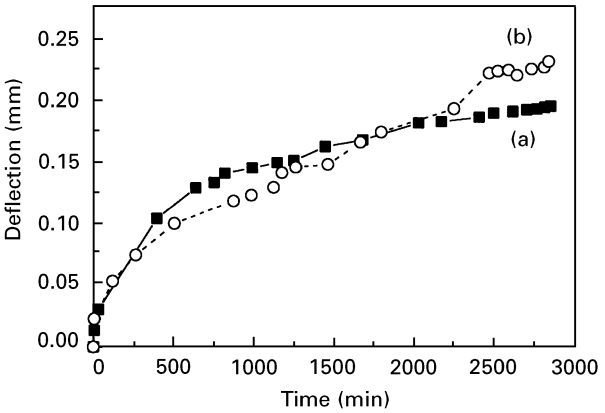

Figure 7 Deflection–time behaviour of (a) composite A and (b) monolithic SiC with the same porosity as composite A, measured at 1100 °C and a bending stress of 100 MPa for 48 h.

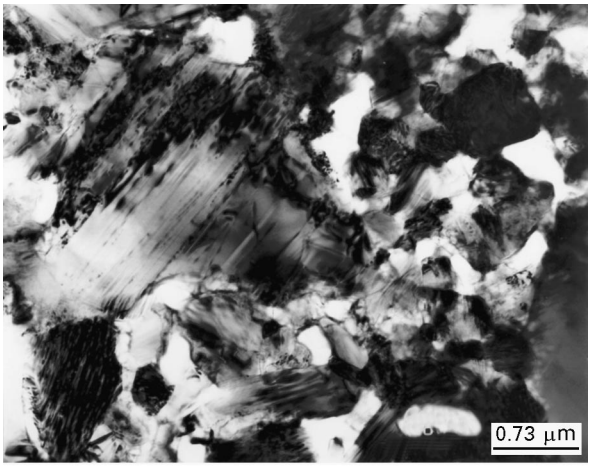

Figure 8 Bright field image of SiC matrix in composite B.

3.2. SiC fibre (18 vol%)/SiC composite fabricated at an applied pressure of 20.7 MPa (composite B)

3.2.1. Microstructure

The microstructure of the matrix, fibre and matrix/fibre interface in composite B was nearly identical to that in composite A except for the level of porosity in the matrix. Thus, the microstructure of composite B will only be briefly discussed. The SiC matrix in composite B was less dense (88 % of theoretical density) than that in composite A, as shown in Fig. 8, because of a lower applied pressure (20.7 MPa) than that (30.0 MPa) in composite A during fabrication. The interfacial layer between the outer carbon layer and matrix consisted of the same phases as composite A, i.e., Al_4C_3, Si–Al–C, and Si–Al–O phases. Also, the Al_2SiO_5 phase was present at a weak interface between the interfacial region and matrix. The interface was weaker than that in composite A, since the matrix in composite B was more porous than that in composite A.

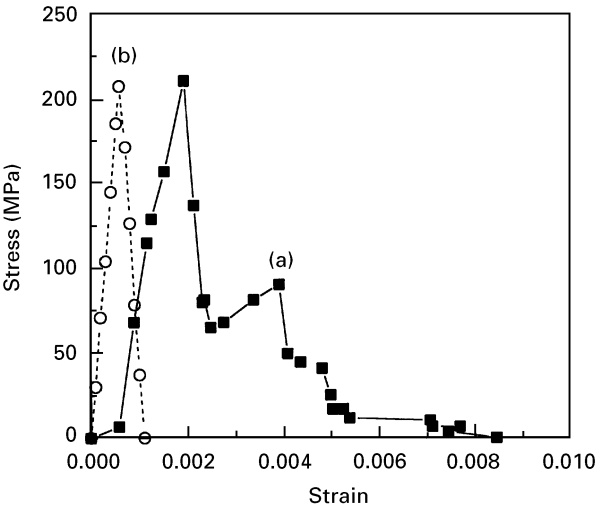

Figure 9 Room-temperature mechanical properties of (a) composite B and (b) monolithic SiC with the same porosity as composite B.

3.2.2. Room-temperature mechanical properties and high-temperature creep properties

Fig. 9 shows the room-temperature mechanical properties of composite B and a monolithic SiC with the same porosity as composite B. The monolithic SiC shows a linear elastic loading up to a brittle fracture, which is a typical mode of ceramics. The fracture strength of composite B is much lower than that of composite A because of the high porosity in the matrix. The pores in composite B act as a fracture-initiating source. The presence of SiC fibre resulted in a substantial increase in the strain to failure over the monolithic SiC because of weak bonding between the interfacial region and outermost carbon sublayer. However, the incorporation could not contribute to an improvement in high-temperature creep properties. This could result from the fact that the fibre could not inhibit the grain boundary sliding in the matrix, owing

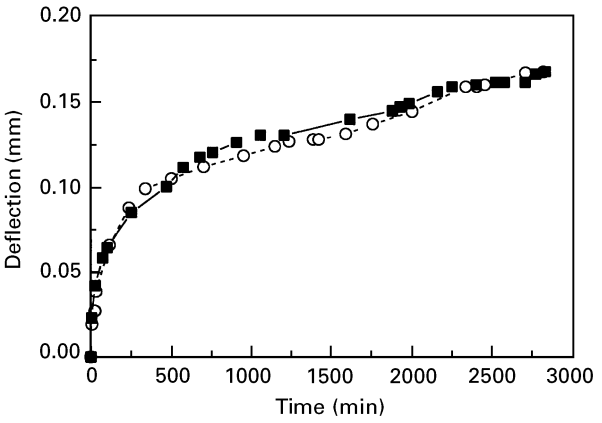

Figure 10 Deflection–time behaviour of (■) composite B and (○) monolithic SiC with the same porosity as composite B measured at 1100 °C and a bending stress of 100 MPa for 48 h.

to high porosity in the matrix. Fig. 10 shows a deflection–time behaviour of composite B and the monolithic SiC with the same porosity as composite B, measured at 1100 °C and a bending stress of 100 MPa for 48 h. This figure shows that the deflection–time

behaviour of composite B is nearly the same as that of the monolithic SiC.

4. Conclusions

In this work, two kinds of SiC (SCS-6™) continuous fibre/SiC composites were fabricated by hot-pressing under different applied pressures of 31.0 and 20.7 MPa in vacuum using 5 wt% Al sintering additive. The composites fabricated at applied pressures of 31.0 and 20.7 MPa during hot-pressing are denoted as composite A and B, respectively. The density and fibre volume fraction of composite A were 3.06 $g\,cm^{-3}$ (97% of theoretical density) and 22%, respectively, and the density and fibre volume fraction of composite B were 2.78 $g\,cm^{-3}$ (88% of theoretical density) and 18%, respectively.

For composite A, a fully dense- and fine-grained SiC matrix contained many twins within the grains. An Al-rich second phase (e.g., Al_2O_3), which was formed at the matrix grain boundaries, was probably responsible for the densification of the SiC powders. It was found that the SiC fibres maintained their original form and microstructure, indicating that no damage occurred during the fabrication. The SiC matrix reacted with the outermost carbon sublayer in the fibre to produce a thin (1.8–4.8 μm) interfacial layer, which consisted of Al_4C_3, Si–Al–C, and Si–Al–O phases. The Al_4C_3 phase was the major phase in the region. The addition of SiC fibre into the SiC matrix resulted in an increase in the room-temperature failure strain and a decrease in the room-temperature fracture strength, relative to the monolithic SiC. In particular, the addition significantly improved the high-temperature creep properties because grain boundary sliding in the matrix was hindered by the fibres and also deformation in the matrix was restrained by the fibres.

The microstructure of the matrix, fibre, and matrix/fibre interface in composite B was basically equivalent to that observed for composite A except for the level of porosity in the matrix. Since the SiC matrix in composite B was less dense (88% of theoretical density) than that in composite A due to lower applied pressure than composite A, the fracture strength of composite B was much lower than that of composite A. The pores in composite B acted as a fracture-initiating flaw, thus significantly decreasing the room-temperature fracture strength. Also, the incorporation could not contribute to the high-temperature creep properties due to the high porosity in the matrix. In conclusion, the Al sintering additive was very efficient for the densification of SiC at a relatively low sintering temperature. This low sintering temperature enables the fibres to maintain their original form and microstructure. It is also necessary to fabricate the SiC fibre/SiC composites under sufficient applied pressure during hot-pressing.

Acknowledgement

We would like to thank Drs. R. C. Krutenat and R. J. Suplinskas of Textron Specialty Materials for helpful discussions and suggestions.

References

1. Brochure produced by Textron Specialty Materials, Lowell, MA 01851, USA.
2. H. TANAKA, Y. INOMATA, K. HARA and H. HASEGAWA, *J. Mater. Sci. Lett.* **4** (1985) 315.
3. D. H. STUTZ, S. PROCHAZKA and J. LORENZ, *J. Amer. Ceram. Soc.* **68** (1985) 479.
4. S. PROCHAZKA and R. M. SCANLAN, *ibid.* **58** (1975) 72.
5. R. A. ALLIEGRO, L. B. COFFIN and J. R. TINKLEPAUGH, *ibid* **39** (1956) 386.
6. F. F. LANGE, *J. Mater. Sci.* **10** (1975) 314.
7. J. M. BIND and J. V. BIGGERS, *J. Appl. Phys.* **47** (1976) 5171.
8. ASTM D790, "Standard Test Methods for Flexural Properties of Unreinforced and Reinforced Plastics and Electrical Insulating Materials", 1995 Annual Book of ASTM Standards Vol. 08.01 (American Society for Testing and Materials, Philadelphia, PA, 1995) p. 155.
9. ASTM E4 "Standard Practices for Force Verification of Testing Machines", 1995 Annual Book of ASTM Standards Vol. 03.01 (American Society for Testing and Materials, Philadelphia, PA, 1995) p. 11.
10. Y. TAJIIMA and W. D. KINGERY, *J. Amer. Ceram. Soc.* **65** (1982) C27.
11. R. HAMMINGER, G. GRATHWOHL and F. THUMMLER, *J. Mater. Sci.* **18** (1983) 3154.
12. X. J. NING and P. PIROUZ, *J. Mater. Res.* **6** (1991) 2234.
13. R. C. KRUTENAT and R. J. SUPLINSKAS, (private communication).
14. A. K. MISRA, *J. Amer. Ceram. Soc.* **74** (1991) 345.
15. T. YANO, S. KATO and T. ISEKI, *ibid* **75** (1992) 580.
16. J. C. VIALA, P. FORTIER and J. BOUIX, *J. Mater. Sci.* **25** (1990) 1842.

Received 13 May
and accepted 2 July 1996